Parkinson's protein α-synuclein : membrane interactions and fibril structure

Kumar, P.

3 Membrane Binding of Parkinson's Protein α-Synuclein: Effect of Phosphorylation at Positions 87 and 129

Kumar P, Schilderink N, Subramaniam V, Huber M. Membrane binding of Parkinson's protein α-Synuclein: Effect of phosphorylation at positions 87 and 129 by the S to D mutation approach. *Israel Journal of Chemistry*, 2016; DOI: 10.1002/ijch.201600083

3.1 Introduction

Parkinson's disease (1) is the second most spread neurodegenerative disease after the Alzheimer's disease (2). This disease is characterized by the formation of protein deposits such as Lewy bodies in the brain (3,4). The protein α-Synuclein (αS) constitutes the main component of these deposits (5–7). A number of post-translational modifications of αS are present within the Lewy bodies in Parkinson's disease (PD) and related disorders (8,9). The major disease-associated post-translational modifications (PTMs) are phosphorylation (8,10), truncation, ubiquitination (11) and also oxidation (like nitration) (12). Phosphorylation is the most studied PTM among them.

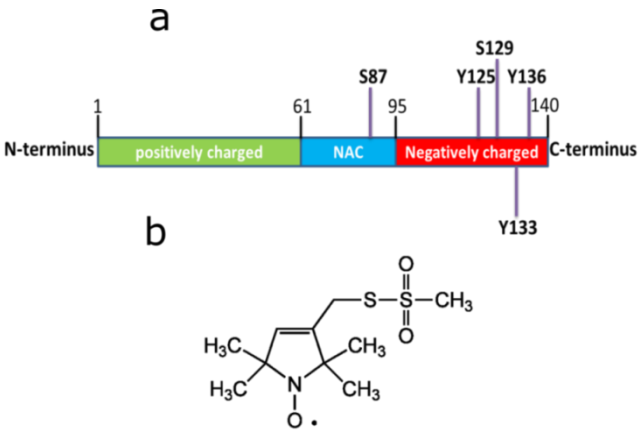

Figure 3.1. a. The most common phosphorylation sites in αS. Given is the sequence number (in boldface) preceeded by the residue (Y or S) that is phosphorylated. Also, the important regions of the protein are shown, indicated by sequence numbers at start and stop. Positively charged (green): Net positive charge of protein between residues 1 and 61, NAC – non-amyloid-β component (blue), and negatively charged C-terminal part of the protein (red), from residue 95 onwards; b. chemical structure of the spin label MTSL, by which Cys is labelled.

The protein αS has been found hyperphosphorylated in Lewy bodies and Lewy neurites (1,9,13). The role of phosphorylation of αS in neurotoxicity is

controversial. However, growing evidence suggests that phosphorylation could influence membrane/vesicle binding of αS and its aggregation(8,14–17). Recent reviews summarize results of in vivo and in vitro studies and describe to which degree phosphorylation of αS is linked to disease (18,19). The major phosphorylation sites of αS are shown in Figure 3.1.

The phosphorylation sites Y125, S129, Y133, and Y136 are most discussed in the literature, for example S129 is highly phosphorylated in Lewy bodies. One more phosphorylation site is special, S87, since it distinguishes the human αS sequence from that of mouse and rat (13). Also, a link between phosphorylation at site 87 and disease was discussed by Paleologou *et al*. (13).

Here we focus on the membrane-binding aspect of αS phosphorylation in vitro at positions S87 and S129. Membrane-binding of αS concerns an amphipathic helix spanning residues from 1-100 (20–22). The N-terminal half (residues 1-50) of the amphipathic helix is termed helix 1, and the other half (residues 51-100), helix 2. The affinity of αS to membranes depends on the negative charge density (ρ) of the membrane, where ρ represents the molar fraction of anionic lipids present in the membrane (23). Different binding properties were found for helix 1 and helix 2 (24).

There are three ways to generate protein constructs to study the effect of phosphorylation: a. to phosphorylate the respective residues enzymatically, which requires dedicated enzymes/ overexpression systems (25,26) and is reversible, b. by a semisynthetic approach in which a (phosphorylated) peptide is linked to the corresponding overexpressed protein (27), and c. by generating mutants whose side chains mimic the chemical properties of the phosphorylated state (negative charge) and size, sometimes referred to as pseudophosphorylation (28). Typically,

serine (S) is replaced by aspartate (D) or glutamate (E) (13,17,29,30) to mimic phosphorylation and alanine (A) is used as reference for the non-phosphorylated state, especially for in vivo studies.

All three approaches have been used to study αS-phosphorylation in vivo and in vitro, showing that in some cases, enzymatically phosphorylated αS (P-αS) and pseudophosphorylated αS behave differently (29,31). For example, enzymatic phosphorylation of αS at S129 has been shown to have an inhibitory effect on αS-aggregation, while pseudophosphorylation does not show such an effect (29). Apparently, the different behavior depends strongly on the properties probed and the environment αS is exposed to. In the present study we focus on the phosphomimic approach with the S→D substitution to mimic phosphorylation, and investigate the constructs S87A or S129A : non-phosporylated; S87D or S129D : phosphorylated.

We used large unilamellar vesicles (LUVs) (see appendix A) as membrane models with a 1:1 mixture of the lipids 1-palmitoyl-2-oleoyl-*sn*-glycero-3-phospho-(1′-rac-glycerol) (POPG) and 1-palmitoyl-2-oleoyl-*sn*-glycero-3-phosphocholine (POPC), generating a membrane with a charge density ρ = 0.5. Previous studies on model membranes showed that at high charge densities, i.e., above 0.8 – 0.9, αS is fully bound to those membranes (23,24,32–34), revealing that the interaction is strong and dominated by electrostatics, which risks to mask the effects of phosphorylation. Additionally, such charge densities are non-physiological, so we avoided these high negative charge densities. At low charge densities ($\rho \leq 0.2$), i.e., on neutral or weakly negatively charged membranes, binding is very low, resulting in a large fraction of unbound protein, which would also abolish any differential binding effect of phosphorylation. This made ρ = 0.5 an optimum charge density to work at.

To investigate membrane binding, we used spin label Electron Paramagnetic Resonance (EPR) spectroscopy. For spin labelling, the amino-acid residue at the sequence position of interest is replaced by a cysteine, which is reacted with a suitable functional group of the nitroxide spin label (see Fig. 1b), an approach introduced by the Hubbell group (35). In this way, a nitroxide, which contains an unpaired electron and is therefore EPR active, is covalently attached to the protein. Then the properties of the protein can be probed at the modified position by EPR. In the present study, we make use of the ability of EPR to detect the mobility of the spin label by room-temperature, continuous-wave (cw) EPR. Characteristic lineshapes of the spectra reveal the mobility of the spin label, with narrow lines corresponding to fast motion (i.e., rotational correlation times (τ_r) of several hundreds of ps) and broad lines to slow motion, in the ns-regime. In our particular case, slow motion of the spin label shows that the section of the protein to which the spin label is attached is bound to the membrane, whereas fast motion shows detachment of the protein from the membrane. The methodology described was introduced before and has proven valuable to determine the local binding of αS to membranes (24,32–34).

The spin-labelled constructs are referred to as *SLposition*αS/S87A(D) or *SLposition*αS/S129A(D), such that for example, SL27αS/S87D is the construct with the spin label at position 27 and is the phosphorylated variant at position 87. We investigated several spin-label positions for each phosphorylation site, resulting in a total of nine constructs, summarized in Table 3.1.

In this work, we show how phosphorylation affects the binding of αS to the membrane. It decreases the binding of αS to the membrane when phosphorylated at the S87 position, whereas no effect is seen when phosphorylated at the S129 position. We also show that phosphorylation at position 87 does not detach the

protein completely from the membrane, but rather causes local unbinding, which is particularly pronounced in the helix 2 region.

3.2 Materials and methods

3.2.1 Protein expression and labelling

All αS mutants were expressed in Escherichia coli strain BL21(DE3) using the pT7-7 expression plasmid and purified in the presence of 1 mM DTT as previously reported(36,37) Serine-87 is substituted either by Alanine (S87A, represents phosphorylation- inactive form) or by Aspartate (S87D, represents phosphomimic form). For labelling, a cysteine mutation was introduced at the desired residues.

Spin labelling was done following the standard protocol, described briefly. Before starting labelling, αS cysteine mutants were reduced with a six-fold molar excess per cysteine with DTT (1,4-dithio-D-threitol) for 30 min at room temperature. To remove DTT, samples were passed through a Pierce Zeba 5 ml desalting column. Immediately, a ten-fold molar excess of the MTSL spin label [(1-oxyl-2,2,5,5-tetramethylpyrroline-3-methyl))-methanethiosulfonate] was added (from a 25 mM stock in DMSO) and incubated for 1 h in the dark at room temperature. After this, free spin label was removed by using two additional desalting steps. Protein samples were applied onto Microcon YM-100 spin columns to remove any precipitated and/or oligomerised proteins and diluted in buffer (10 mM Tris-HCl, pH 7.4). Spin label concentrations were 2.5 mM at protein concentrations of 250 µM. Owing to the high reactivity of the label and the fact that the cysteine residues are freely accessible in the poorly folded structure, near quantitative labelling can be achieved under these conditions(38). Samples were stored at -80 ^{o}C.

3.2.2 Preparation of vesicles

All lipids were purchased from Avanti Polar Lipids, Inc. as chloroform solutions and were used without further purification. LUVs were prepared from 1 : 1 mixtures of 1-palmitoyl-2-oleoyl-*sn*-glycero-3-phospho-(1′-rac-glycerol) (POPG) and 1-palmitoyl-2-oleoyl-*sn*-glycero-3-phosphocholine (POPC). Lipids were mixed in the desired ratio and then chloroform was evaporated by dry nitrogen gas. The resulting lipid films were kept under vacuum overnight. Dried lipid films were hydrated with 10 mM Tris – HCl, pH 7.4 for 1 hour at 30 ^{o}C, and the resulting milky lipid suspensions were extruded through 100 nm pore size polycarbonated membranes using the mini extruder (catalogue no. 610000) from Avanti Polar Lipids. The size of the vesicles was determined by dynamic light scattering (DLS). The DLS-experiments were performed on a Zetasizer Nano-ZS (Malvern). We obtained vesicles with a homogeneous size distribution around diameter d = 100 nm.

3.2.3 Sample Preparation

Spin-labelled αS mutants were added from stock solutions (concentration between 150 µM and 250 µM) to the LUVs to obtain a lipid to protein ratio (L : P) of 250 : 1, and incubated for 30 min at room temperature before measuring. All samples were prepared and measured at least three times. All spin labelled αS constructs used in this work are shown in Table 3.1.

3.2.4 Filtration experiments

To determine, whether αS physically detaches from the membrane, we performed filtration experiments similar to those described in Drescher et. al (24). An αS-vesicle solution, prepared as for the EPR experiments described above

(sample preparation), was passed through a 100 kDa cut-off filter device (Amicon Ultra 100k), which retains the vesicles and thereby the membrane-bound αS fraction, but is permeable for unbound αS. The concentration of αS in the filtrate is too low to measure directly, therefore the filtrate was concentrated using a 3 kDa cut-off filter device (Amicon Ultra 3k) and measured by EPR to determine the amount of αS in the filtrate. The error in the final value, in the order of 20 %, derives largely from the errors in determining the volumes before and after the concentration step, and the error of the double integral procedure to determine the spin concentration by EPR.

Table 3.1. The αS constructs used to study phosphorylation at position S87 and S129; SL denotes the spin-label.

Spin label positions	**S87A (non-phosphorylated)**	**S87D (phosphorylated)**
SL27	SL27αS/S87A	SL27αS/S87D
SL56	SL56αS/S87A	SL56αS/S87D
SL63	SL63αS/S87A	SL63αS/S87D
SL69	SL69αS/S87A	SL69αS/S87D
SL76	SL76αS/S87A	SL76αS/S87D
SL90	SL90αS/S87A	SL90αS/S87D
Spin label positions	**S129A (non-phosphorylated)**	**S129D (phosphorylated)**
SL27	SL27αS/S129A	SL27αS/S129D
SL56	SL56αS/S129A	SL56αS/S129D
SL69	SL69αS/S129A	SL69αS/S129D

3.2.5 Continuous wave-EPR experiments

The 9.7 GHz continuous-wave (cw) EPR measurements have been performed using an ELEXSYS E680 spectrometer (Bruker, Rheinstetten, Germany) with a Super high Q cavity (ER 4122 SHQE-W1/1108). Measurements were performed at

20 ^{o}C, using 0.63 mW of microwave power, 100 kHz modulation frequency and a modulation amplitude of 0.1 mT. Total acquisition time for the EPR spectra was 20 minutes.

3.2.5.1 Simulation of cw-EPR spectra

Spectral simulations were performed using Matlab (7.11.0.584, Natick, Massachusetts, U.S.A) and the EasySpin package(39). For all simulations, the following spectral parameters were used: g = [2.00906, 2.00687, 2.00300] (40), the hyperfine tensor parameters $A_{xx} = A_{yy} = 13$ MHz, and A_{zz} was varied (see Table 3.2). Usually a superposition of more than one component was required to simulate the spectra. The parameters were manually changed to check in which range acceptable simulations of the experimental spectra were obtained to determine the error margins. To simulate spectra of αS bound to membranes, the τ_r of the fastest component was kept at the τ_r value of the spectra of the respective protein construct in the absence of vesicles.

3.3 Results

We investigate the binding of phosphorylation variants of αS at positions 87 and 129 to LUVs of 100 nm diameter. The LUVs are composed of a 1:1 mixture of POPG and POPC, generating a membrane of charge density ρ = 0.5. We first describe the results of phosphorylation at position 87, then at 129.

Figure 3.2 shows the spectra of the spin labelled constructs probing phosphorylation at position 87 in the presence of LUVs (for complete list of constructs, see Table 3.1). In this set, helix 1 is probed in the middle, at residue 27, helix 2 is probed at five positions starting from position 56 and terminating in 90. Figure 3.22a shows the spectra of αS in the non-phosphorylated and Figure 3.2b

in the phosphorylated form. Spectra in Figure 3.2a differ from those in Figure 3.2b, most notably, each spectrum in Figure 3.2b has narrower lines than its counterpart in Figure 3.2a. As described in the introduction, narrow lines derive from spin-labels that are rotating fast. As discussed in more detail below, fast rotation shows that the section of the protein to which the spin label is attached is not bound to the membrane. More detailed information was obtained by spectral simulation of the experimental spectra, which yields the parameters of mobility of the spin label, the rotational correlation time (τ_r) and, in the case of multicomponent spectra, the amount by which each fraction contributes. These parameters are given in Table 3.2. In Fig. 2c, an example of a simulation is shown. Three fractions are visible, the fast, the slow and the immobile component, which have increasingly large linewidths. The individual components add up to give the experimental spectrum. Table 3.2 reveals that all but two spectra consist of a superposition of two components, the fast and slow components, except for the SL56αS/S87A variant, which in addition has a third, the immobile component, and the SL90αS/S87A and SL90αS/S87D variants, which have only one component, the fast component. Each component reflects a part of the protein population: The fast fraction is due to protein in which the region around the site that is spin labelled is not attached to the membrane, whereas the slow and immobilized fractions are due to sections bound to the membrane. The amount by which each component contributes to the spectra (Table 3.2, columns four and six) reflects the fraction of protein contributing to each component. The correlation times can be determined to several tens of ps, in the case of the fast fraction, and several hundreds of ps for the slow fraction (see Table 3.2). The contribution of the fast component of αS in the non-phosphorylated form is smaller than in the phosphorylated form for each probing position. The opposite is the case for the

contribution of the slow components. Both these trends reveal that phosphorylation reduces membrane binding.

To illustrate the effect of phosphorylation at position 87, Figure 3.3 shows a plot of the amount of the fast fraction for phosphorylation at position 87 as a function of the sequence number at which mobility is probed. For all monitoring positions, the amount of mobile fraction is larger in the phosphorylated variant. At monitoring positions 27 and 56, the amount of mobile fractions of non-phosphorylated αS is below 10 %, which indicates strong binding, but at later positions (helix 2) the amount of fast fractions increases to 70 % indicating the loosening of the helix 2 of αS, when it is non-phosphorylated, in agreement with previous findings for wt αS (24). For the phosphorylated αS, the amount of the mobile fraction is higher than in the non-phosphorylated form for all positions monitored, enhancing the tendency for local unbinding in helix 2 until, at position 90, the bound fraction so low that it becomes undetectable.

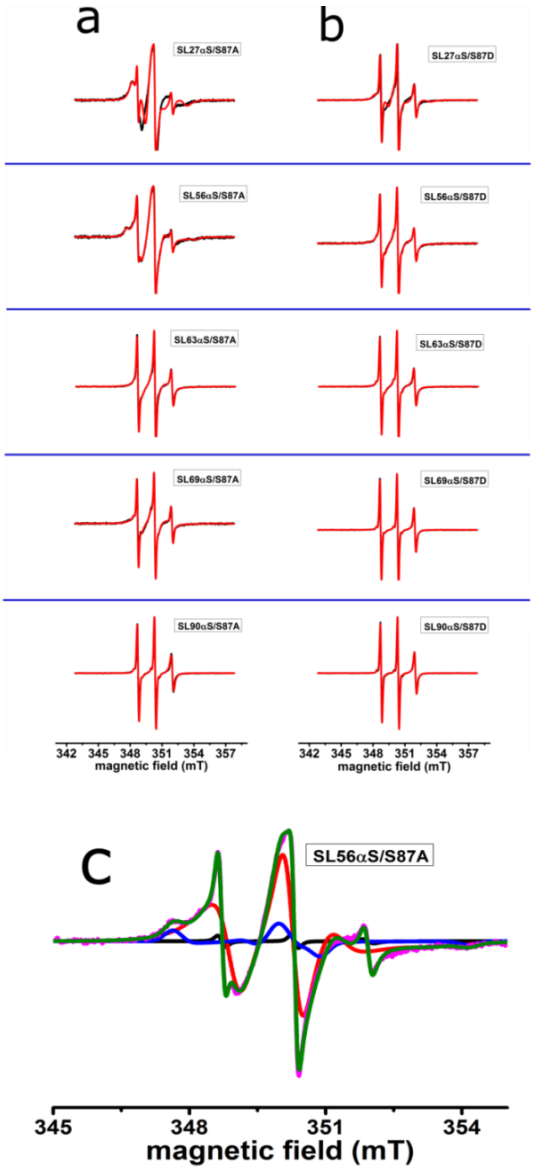

Figure 3.2. Effect of phosphorylation at position 87 on αS-binding to LUVs: Room temperature, EPR spectra of spin-labelled αS constructs (for nomenclature see Table 3.1) with LUVs of a 1:1 mixture of POPG and POPC; a. non-phosphorylated b. phosphorylated form. Black line: experiment, red line: simulation. c. Decomposition of EPR spectrum into components shown for SL56αS/S87A. The fast (black), slow (red) and immobilized (blue) components are shown as well as the added simulation (green) and the experimental spectrum (pink).

Table 3.2. Effect of phosphorylation of αS at position 87 (S87A/D): Parameters describing the mobility of the spin label in the EPR spectra; τ_r rotation correlation time of the spin label, A_{zz}, the hyperfine splitting along the Z-direction.

αS spin-label positions	components contributing to spectra	S87A (non- phosphorylated)			S87D (phosphorylated)		
		τ_r (ns)	contribution (%)	A_{zz} (MHz)	τ_r (ns)	Contribution (%)	A_{zz} (MHz)
SL 27	fast	0.4 ± 0.03	6 ± 0.4	110	0.4 ± 0.02	32 ± 2	110
	slow	8.5 ± 0.2	94 ± 0.4	85	9.3 ± 0.65	67 ± 2	83
	immobile	na	na	na	na	na	na
SL 56	fast	0.4 ± 0.02	6 ± 0.2	110	0.4 ± 0.03	34 ± 3	110
	slow	3.2 ± 0.07	78 ± 1.2	102	3.1 ± 0.4	63 ± 3	102
	immobile	>50	16 ± 1	91	na	na	na
SL 63	fast	0.35 ± 0.04	29 ± 2	110	0.4 ± 0.03	51 ± 5	110
	slow	2.6 ± 0.3	70 ± 2	105	2.5 ± 0.6	44 ± 5	108
	immobile	na	na	na	na	na	na
SL 69	fast	0.3 ± 0.02	23 ± 2	110	0.3 ± 0.02	75 ± 9	110
	slow	2.5 ± 0.2	75 ± 2	110	2.5 ± 1.2	20 ± 9	110
	immobile	na	na	na	na	na	na

SL 76	fast	0.4 ± 0.04	42 ± 5	110	0.4 ± 0.02	79 ± 8	110
	slow	3.5 ± 0.8	57 ± 5	110	3.5 ± 3.2	16 ± 8	110
	immobile	na	na	na	na	na	na
SL 90	fast	0.4 ± 0.04	70 ± 10	110	0.3 ± 0.03	100* ± 8	110
	slow	2.5 ± 1.3	24 ± 10	110	na	na	na
	immobile	na	na	na	na	na	na

na: A component seen in other spectra, but not required to obtain a good simulation of the experimental spectrum in question, revealing that the rotational correlation time of the spin label does not contain contributions on the time scale of the component in question (for details see text and Fig. 2). For error determination see Materials and methods. *including 4.5 % contribution of spin label with natural abundance of ^{13}C.

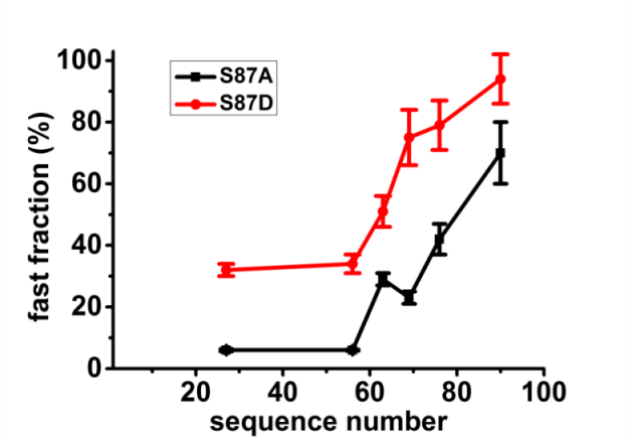

Figure 3.3. Local unbinding effect of phosphorylation at position 87: Amount of fast fraction in αS 87 A, D mutants in the presence of LUVs as a function of the sequence number. black: non-phosphorylated (αS87A), red: phosphorylated (αS87D) (see Table 3.2 for values), the lines connecting the points are guides to the eye.

To determine if the phosphorylation reduces the overall membrane affinity of αS, i.e., if αS detaches completely from the membrane, resulting in αS protein that is

free in solution (physical unbinding) we separated the unbound fraction of αS from the membrane-bound fraction, by filtrating the sample through a filter that retains the vesicles and αS bound to them. The amount of physically unbound protein in the filtrate is then determined by EPR, as described in Drescher et al. (24) (for details see Materials and methods). The amount of unbound αS is given in Table 3.3 and is below 16 % for all constructs. Thus the amount of physically unbound αS is significantly lower than the amount of the fast fraction measured by EPR (see Table 3.2), showing that the local unbinding far out-weighs any physical unbinding. The percentages in Table 3.3 for spin label positions 27 and 56 are slightly lower than for the other positions. Given that the differences are just outside the error margins of the procedure, we cannot draw conclusions.

Table 3.3. Physical unbinding of αS S87D from the membrane. Results of filtration experiments (for details, see Materials and methods and also Results).

mutants	αS unbound fraction (%)
SL27αS/S87D	5.9 ± 2.0
SL56αS/S87D	5.2 ± 1.0
SL69αS/S87D	15.1 ± 3.0
SL90αS/S87D	13.6 ± 3.0

For phosphorylation at position 129, Figure 3.4 shows the superposition of the spectra of non-phosphorylated and phosphorylated variants for three spin label positions (see Table 3.1). In contrast to phosphorylation at position 87, A and D variants at position 129 have similar spectra, obviating the need for detailed spectral analysis. Apparently, phosphorylation has a much smaller influence at position 129 than at position 87.

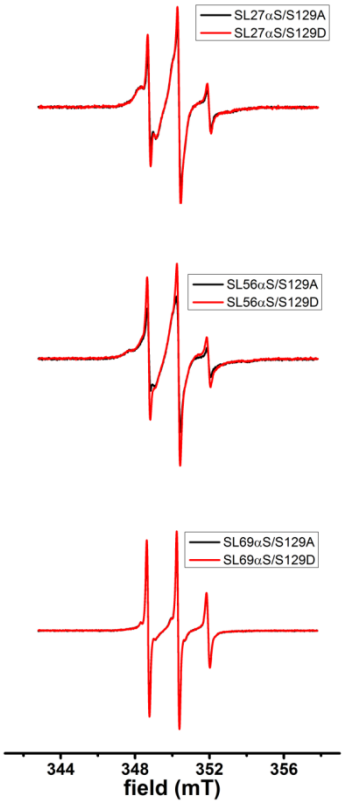

Figure 3.4. Effect of phosphorylation at position 129 on αS-binding to LUVs: Room temperature, EPR spectra of spin-labelled αS constructs (for nomenclature see Table 3.1) with LUVs of a 1:1 mixture of POPG and POPC; Superposition of non-phosphorylated (black line) with phosphorylated EPR spectra (red line), normalized by their double integral value.

3.4 Discussion

We have investigated how membrane binding of αS depends on the phosphorylation state of positions 87 and 129. Membrane binding is detected locally, via the mobility of spin labels attached to specific positions in the protein. An increased spin-label mobility shows that the protein detaches from the membrane around the position probed.

The membrane composition was chosen to be conducive to intermediate binding with a charge density of ρ = 0.5, to avoid: a) dominant electrostatic effects observed at higher charge densities, where they cause strong, undifferentiated binding and are non-physiological, b) overall unbinding observed at low charge densities (23,24,32–34), as described in the introduction. The membrane was offered in the form of LUVs of a diameter of 100 nm. We mimic phosphorylation by the phosphorylation-mutation approach, replacing S by D, an approach used before (13,17,29,30) (for details, see introduction). Although some studies showed that biochemically phosphorylated αS can have different properties than phosphorylation mimics (29,31), the latter constructs provide a robust system to study phosphorylation effects in vitro, explaining their popularity.

Under the conditions of our study, phosphorylation at position 129 has no noticeable effect on membrane binding, whereas 87 has, similar to what was observed by other techniques in the past (13). In the following, we will first discuss the influence of phosphorylation at position 87 on αS-membrane binding, and then compare the results obtained on both phosphorylation sites to previous findings in the literature.

When position 87 is phosphorylated, membrane binding is reduced relative to the non-phosphorylated case. An almost the same reduction of the binding is observed at positions 27 and 56 in the helix 1 region, see Figure 3.3. Similar to wild type αS (24), also in the S87A variants, helix 2 has a lower membrane affinity than helix 1. Phosphorylation enhances this trend, up to the point that at probing position 90, the bound fraction becomes so low that it is undetectable. Complete, detachment of the phosphorylated protein from the membrane does not play a role: as seen in Table 3.3, the physically unbound fraction is below 16 % for all constructs. To place this into perspective, the amount of physically unbound αS is

maximally one third of the amount of fast fraction determined from EPR, showing that the majority of the fraction, seen by EPR, derives from protein that is attached to the membrane, presumably at the residues preceding the probed sequence position, e.g. for sample SL27/αS87P, residues 27 and below.

Fluctuations in the amount of fast fraction (Table 3.2, SL 63, non-phosphorylated (SL63/S87A) has a larger amount of fast fraction than SL 69) and a larger amount of physically unbound αS for SL positions in helix 2 (Table 3.3), could indicate an influence of the spin label on αS-membrane binding. If such an effect is present, it never exceeds a contribution of 10 %, and therefore is not relevant for the conclusions drawn.

Overall we find that phosphorylation at position 87 decreases the membrane affinity of αS, more for helix 2. This effect is fully consistent with the change in the charge caused by the conversion of S→D or by phosphorylation: A negative charge in the helix 2 will weaken the electrostatic interaction with the negatively charged membrane surface as it counteracts the effect of several lysines (Lys;K) in the αS sequence from residues 1-100. Reduced membrane binding of S87E and P-S87 has been reported before, e.g. (13) (41).

Reduced membrane binding affects the entire protein, but is most pronounced in the helix 2 region, and may selectively influence the behavior of helix 2. Some models propose that the physiological function of αS involves vesicle fusion events in which helix 1 and helix 2 interact with different types of membranes (42). We therefore speculate that phosphorylation at position 87 could be used to tune how αS operates in vesicle trafficking.

For the αS129 A/D variants, the difference in mobility of the spin label for phosphorylated and non-phosphorylated forms is minute, showing that under the

membrane conditions employed here, phosphorylation at this site does not affect membrane binding. The C-terminus of αS is already negatively charged and was not found to interact with the membrane in previous studies (20,21,24,38,43), which is fully consistent with the lack of changes in membrane-binding observed in the present study upon phosphorylation at position 129.

The results of the present study suggest that phosphorylation at position 87 tunes those functions of αS that involve membrane binding and vesicle interaction, whereas phosphorylation at position 129 acts on other aspects of αS in the organism. Previously (13) several possibilities of how phosphorylation at position 129 could affect αS in vivo behavior are described and the study of Kosten et.al (44) shows that the phosphorylation at position 129 depends on the phosphorylation state of position 125, suggesting a complex interplay of posttranslational modifications in the C-terminus.

Most of the current research is focused on phosphorylation at position 129, and the phosphorylation degree at this position is related to disease effects, as reviewed in (45). In agreement with our results, several studies show that αS phosphorylation at 129 has no or little effect on membrane binding, see for example (28). However, several studies find an influence of phosphorylation at 129 on the aggregation of αS (28,29,46) and on membrane binding of αS aggregates (46) suggesting that in vivo effects are linked to aggregation-sensitive processes.

In conclusion, the large spectrum of phosphorylation effects on αS in vivo and in vitro (13–16,19,28–31,41,45–54) furnishes the need for isolating the different factors that can be modulated by αS phosphorylation in vitro. The present study gives one such example, where we show that in vitro-phosphorylation mimics at

position 87 (S87D) reduce αS-membrane binding in a local, sequence dependent manner, whereas the same modification at position 129 (S129D) has no influence on membrane binding. We expect that this approach provides a foothold to interpret the challenging in vivo physiological and pathological functions of αS.

3.5 References

1. Parkinson J. An Essay on the Shaking Palsy (Whitingham and Rowland, London). 1817.
2. De Rijk MC, Breteler MM, Graveland GA, Ott A, Grobbee DE, van der Meché FG, Hofman A. Prevalence of Parkinson's disease in the elderly: the Rotterdam Study. Neurology. 1995;45:2143–2146.
3. Junn E, Ronchetti RD, Quezado MM, Kim S-Y, Mouradian MM. Tissue transglutaminase-induced aggregation of alpha-synuclein: Implications for Lewy body formation in Parkinson's disease and dementia with Lewy bodies. Proc Natl Acad Sci U S A. 2003;100:2047–2052.
4. Chung KK, Zhang Y, Lim KL, Tanaka Y, Huang H, Gao J, Ross CA, Dawson VL, Dawson TM. Parkin ubiquitinates the alpha-synuclein-interacting protein, synphilin-1: implications for Lewy-body formation in Parkinson disease. Nat Med. 2001;7:1144–1150.
5. Spillantini MG, Schmidt ML, Lee VM, Trojanowski JQ, Jakes R, Goedert M. Alpha-synuclein in Lewy bodies. Nature. 1997;388:839–840.
6. Spillantini MG, Crowther RA, Jakes R, Hasegawa M, Goedert M. α-Synuclein in filamentous inclusions of Lewy bodies from Parkinson's disease and dementia with Lewy bodies. Proc Natl Acad Sci U S A. 1998;95:6469–6473.
7. Goedert M. Alpha-synuclein and neurodegenerative diseases. Nat Rev Neurosci. 2001;2: 492–501.
8. Fujiwara H, Hasegawa M, Dohmae N, Kawashima A, Masliah E, Goldberg MS, Shen J, Takio K, Iwatsubo T. α-Synuclein is phosphorylated in synucleinopathy lesions. Nat Cell Biol. 2002;4:160–164.
9. Anderson JP, Walker DE, Goldstein JM, De Laat R, Banducci K, Caccavello RJ, Barbour R, Huang J, Kling K, Lee M, Diep L, Keim PS, Shen X, Chataway T, Schlossmacher MG, Seubert P, Schenk D, Sinha S, Gai WP, Chilcote TJ.

Phosphorylation of Ser-129 is the dominant pathological modification of α-Synuclein in familial and sporadic Lewy body disease. J Biol Chem. 2006;281:29739–29752.

10. Okochi M, Walter J, Koyama a, Nakajo S, Baba M, Iwatsubo T, Meijer L, Kahle PJ, Haass C. Constitutive phosphorylation of the Parkinson's disease associated α-Synuclein. J Biol Chem. 2000;275:390–397.

11. Shimura H, Schlossmacher M, Hattori, N.Frosch M, Trockenbacher A, Schneider R, Mizuno Y, Kosik KS, Selkoe DJ. Ubiquitination of a new form of α-Synuclein by parkin from human brain: implications for Parkinson's disease. Science. 2001;293:263–269.

12. Hodara R, Norris EH, Giasson BI, Mishizen-Eberz AJ, Lynch DR, Lee VM, Ischiropoulos H. Functional consequences of α-Synuclein tyrosine nitration: diminished binding to lipid vesicles and increased fibril formation. J Biol Chem. 2004;279:47746–47753.

13. Paleologou KE, Oueslati A, Shakked G, Rospigliosi CC, Kim H-Y, Lamberto GR, Fernandez CO, Schmid A, Chegini F, Gai WP, Chiappe D, Moniatte M, Schneider BL, Aebischer P, Eliezer D, Zweckstetter M, Masliah E, Lashuel HA. Phosphorylation at S87 Is enhanced in synucleinopathies, inhibits α-Synuclein oligomerization, and influences Synuclein-membrane interactions. J Neurosci. 2010;30:3184–3198.

14. Gorbatyuk OS, Li S, Sullivan LF, Chen W, Kondrikova G, Manfredsson FP, Mandel RJ, Muzyczka N. The phosphorylation state of Ser-129 in human α-Synuclein determines neurodegeneration in a rat model of Parkinson disease. Proc Natl Acad Sci U S A. 2008;105:763–768.

15. McFarland NR, Fan Z, Xu K, Schwarzschild MA, Feany MB, Hyman BT, McLean PJ. α-Synuclein S129 phosphorylation mutants do not alter nigrostriatal toxicity in a rat model of Parkinson disease. J Neuropathol Exp Neurol. 2009;68:515–524.

16. Smith WW. α-Synuclein phosphorylation enhances eosinophilic cytoplasmic inclusion formation in SH-SY5Y cells. J Neurosci. 2005;25:5544–5552.

17. Chen L, Feany MB. α-Synuclein phosphorylation controls neurotoxicity and inclusion formation in a Drosophila model of Parkinson disease. Nat Neurosci. 2005;8:657–663.

18. Tenreiro S, Eckermann K, Outeiro TF. Protein phosphorylation in neurodegeneration: Friend or foe? Front Mol Neurosci. 2014;7:1-30.

19. Sato H, Kato T, Arawaka S. The role of Ser129 phosphorylation of α-Synuclein in neurodegeneration of Parkinson's disease: A review of in vivo models. Rev Neurosci. 2013;24:115–123.

20. W S Davidson, A Jonas, D F Clayton JMG. Stabilization of α-Synuclein secondary structure upon binding to synthetic membranes. J Biol Chem. 1998;273:9443–9449.

21. Eliezer D, Kutluay E, Bussell R, Browne G. Conformational properties of α-Synuclein in its free and lipid-associated states. J Mol Biol. 2001;307:1061–1073.

22. Jao CC, Hegde BG, Chen J, Haworth IS, Langen R. Structure of membrane-bound α-Synuclein from site-directed spin labeling and computational refinement. Proc Natl Acad Sci U S A. 2008;105:19666–19671.

23. Middleton ER, Rhoades E. Effects of curvature and composition on α-Synuclein binding to lipid vesicles. Biophys J. 2010;99:2279–2288.

24. Drescher M, Godschalk F, Veldhuis G, van Rooijen BD, Subramaniam V, Huber M. Spin-label EPR on α-Synuclein reveals differences in the membrane binding affinity of the two antiparallel helices. ChemBioChem. 2008;9:2411–2416.

25. Burnett G, Kennedy EP. The enzymatic phosphorylation of proteins. J Biol Chem. 1954; 211:969–980.

26. Kresge N, Simoni RD, Hill RL. The process of reversible phosphorylation: The work of Edmond H. Fischer. J Biol Chem. 2011;286:e1–e2.

27. Hejjaoui M, Butterfield S, Fauvet B, Vercruysse F, Cui J, Dikiy I, Prudent M, Olschewski D, Zhang Y, Eliezer D, Lashuel HA. Elucidating the role of C-terminal post-translational modifications using protein semisynthesis strategies: α-Synuclein phosphorylation at tyrosine 125. J Am Chem Soc. 2012;134:5196–5210.

28. Nübling GS, Levin J, Bader B, Lorenzl S, Hillmer A, Högen T, Kamp F, Giese A. Modelling Ser129 phosphorylation inhibits membrane binding of pore-forming α-Synuclein oligomers. PLoS One. 2014;9:1-7.

29. Paleologou KE, Schmid AW, Rospigliosi CC, Kim H-Y, Lamberto GR, Fredenburg RA, Lansbury Jr PT, Fernandez CO, Eliezer D, Zweckstetter M, Lashuel HA. Phosphorylation at Ser-129 but not the phosphomimics S129E/D inhibits the fibrillation of α-Synuclein. J Biol Chem. 2008;283:16895–16905.

30. Chen L, Periquet M, Wang X, Negro A, Mclean PJ, Hyman BT, Feany MB. Tyrosine and serine phosphorylation of α-Synuclein have opposing effects on neurotoxicity and soluble oligomer formation. J Clin Invest. 2009;119:3257–3265.

31. Schreurs S, Gerard M, Derua R, Waelkens E, Taymans J-M, Baekelandt V, Engelborghs Y. In Vitro phosphorylation does not influence the aggregation kinetics of WT α-Synuclein in contrast to its phosphorylation mutants. Int J Mol Sci. 2014;15:1040–1067.

32. Robotta M, Hintze C, Schildknecht S, Zijlstra N, Jüngst C, Karreman C, Huber M, Leist M, Subramaniam V, Drescher M. Locally resolved membrane binding affinity of the N-terminus of α-Synuclein. Biochemistry. 2012;51:3960–3962.

33. Robotta M, Gerding HR, Vogel A, Hauser K, Schildknecht S, Karreman C, Leist M, Subramaniam V, Drescher M. Alpha-Synuclein binds to the inner membrane of mitochondria in an α-helical conformation. Chembiochem. 2014;1–4.

34. Kumar P, Segers-Nolten IMJ, Schilderink N, Subramaniam V, Huber M. Parkinson's protein α-Synuclein binds efficiently and with a novel conformation to two natural membrane mimics. PLoS One. 2015;10:1-11.

35. Hubbell WL, Gross A, Langen R, Lietzow MA. Recent advances in site-directed spin labelling of proteins. Curr Opin Struct Biol. 1998;8:649–656.

36. Van Raaij ME, Segers-Nolten IMJ, Subramaniam V. Quantitative morphological analysis reveals ultrastructural diversity of amyloid fibrils from alpha-synuclein mutants. Biophys J.2006;91:L96–L98.

37. Veldhuis G, Segers-Nolten I, Ferlemann E, Subramaniam V. Single-molecule FRET reveals structural heterogeneity of SDS-bound α-synuclein. ChemBioChem. 2009;10:436–439.

38. Jao CC, Der-Sarkissian A, Chen J, Langen R. Structure of membrane-bound α-Synuclein studied by site-directed spin labeling. Proc Natl Acad Sci U S A. 2004;101:8331–8336.

39. Stoll S, Schweiger A. EasySpin, a comprehensive software package for spectral simulation and analysis in EPR. J Magn Reson. 2006;178:42–55.

40. Steigmiller S, Börsch M, Gräber P, Huber M. Distances between the b-subunits in the tether domain of F0F1-ATP synthase from E. coli. Biochim Biophys Acta-Bioenerg. 2005;1708:143–153.

41. Oueslati A, Paleologou KE, Schneider BL, Aebischer P, Lashuel HA. Mimicking phosphorylation at serine 87 inhibits the aggregation of human α-Synuclein and protects against its toxicity in a rat model of Parkinson's disease. J Neurosci. 2012;32:1536–1544.

42. Dikiy I, Eliezer D. Folding and misfolding of α-Synuclein on membranes. Biochim Biophys Acta - Biomembr. 2012;1818:1013–1018.

43. Ulmer TS, Bax A. Structure and dynamics of micelle-bound human α-Synuclein. J Biol Chem. 2005;280:9595–9603.

44. Kosten J, Binolfi A, Stuiver M, Verzini S, Theillet F-X, Bekei B, van Rossum M, Selenko P. Efficient modification of α-Synuclein serine 129 by protein kinase CK1 requires phosphorylation of tyrosine 125 as a priming event. ACS Chem Neurosci. 2014;5:1203–1208.

45. Oueslati A. Implication of α-Synuclein phosphorylation at S129 in synucleinopathies: What have we learned in the last decade? J Parkinsons Dis. 2016;6:39–51.

46. Samuel F, Flavin WP, Iqbal S, Pacelli C, Sri Renganathan SD, Trudeau LE, Campbell EM, Fraser PE, Tandon A. Effects of serine 129 phosphorylation on α-Synuclein aggregation, membrane association, and internalization. J Biol Chem. 2016;291:4374–4385.

47. Azeredo da Silveira S, Schneider BL, Cifuentes-Diaz C, Sage D, Abbas-Terki T, Iwatsubo T, Unser M, Aebischer P. Phosphorylation does not prompt, nor prevent, the formation of α-Synuclein toxic species in a rat model of Parkinson's disease. Hum Mol Genet. 2009;18:872–887.

48. Braithwaite SP, Stock JB, Mouradian MM. α-Synuclein phosphorylation as a therapeutic target in Parkinson's disease. Rev Neurosci. 2012;23:191–198.

49. Fiske M, Valtierra S, Solvang K, Zorniak M, White M, Herrera S, Konnikova A, Brezinsky R, Deb Burman S, Contribution of alanine-76 and serine phosphorylation in α-Synuclein membrane association and aggregation in yeasts. Parkinsons Dis. 2011;2011:1-12.

50. Ha Y, Yang A, Lee S, Kim K, Liew H, Suh YH, Park HS, Churchill DG. Facile "stop codon" method reveals elevated neuronal toxicity by discrete S87p-α-Synuclein oligomers. Biochem Biophys Res Commun. 2014;443:1085–1091.

51. Kuwahara T, Tonegawa R, Ito G, Mitani S, Iwatsubo T. Phosphorylation of α-Synuclein protein at Ser-129 reduces neuronal dysfunction by lowering its membrane binding property in Caenorhabditis elegans. J Biol Chem. 2012;287:7098–7109.

52. Visanji NP, Wislet-Gendebien S, Oschipok LW, Zhang G, Aubert I, Fraser PE, Tondon A. Effect of Ser-129 phosphorylation on interaction of α-Synuclein with synaptic and cellular membranes. J Biol Chem. 2011;286:35863–35873.

53. Tenreiro S, Reimão-Pinto MM, Antas P, Rino J, Wawrzycka D, Macedo D, Rosado-Ramos R, Amen T, Waiss M, Magalhaes F, Gomes A, Santos CN, Kaganovich D, Outeiro TF. Phosphorylation modulates clearance of α-Synuclein inclusions in a yeast model of Parkinson's Disease. PLoS Genet. 2014;10:1-23.

54. Xu Y, Deng Y, Qing H. The phosphorylation of α-Synuclein: Development and implication for the mechanism and therapy of the Parkinson's disease. J Neurochem. 2015;135:4–18.

Appendix A to Chapter 3

In chapter 3, the effect of phosphorylation of α-Synuclein (αS) on binding to large unilamellar vesicles (LUVs) was studied, here we investigate the interaction of phosphorylated and non-phosphorylated αS with small unilamellar vesicles (SUVs) with the same lipid compositions as used for LUVs, i.e., POPG : POPC = 1 : 1 (charge density ρ = 0.5). We describe the binding of S87 variants of αS at three probing positions (27, 56 and 69) by spin-labeled electron paramagnetic resonance (EPR) spectroscopy.

SUVs were prepared as described in chapter 2. The size of the vesicles was determined by dynamic light scattering (DLS). The DLS-experiments were performed on a Zetasizer Nano-ZS (Malvern). We obtained vesicles with a homogeneous size distribution with a diameter of approximately d = 50 nm.

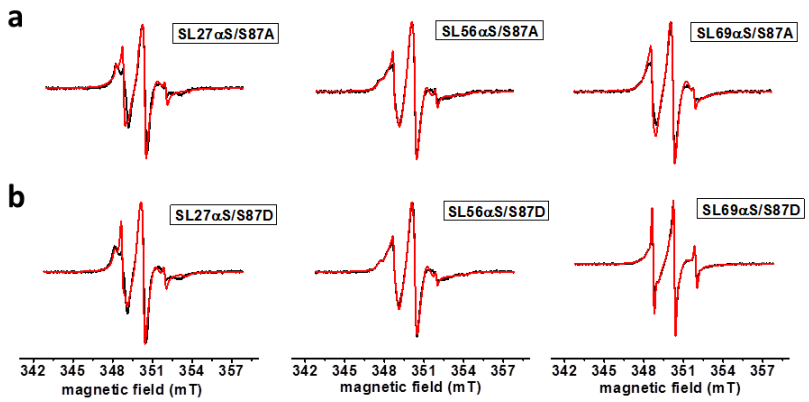

Figure A1. Effect of phosphorylation at position 87 on αS-binding to SUVs: Room temperature, EPR spectra of spin-labeled αS constructs (SL27, 56, and 69) with SUVs of a 1:1 mixture of POPG and POPC; a. non-phosphorylated b. phosphorylated form. Black line: experiment, red line: simulation.

Figure A1 shows the spectra of spin-labeled constructs of αS probing the effect of phosphorylation at position 87 in the presence of SUVs. In this set, helix 1 is probed in the middle, at residue 27, helix 2 is probed at positions 56 and 69.

Table A1. Effect of phosphorylation of αS at position 87 (S87A/D): Parameters describing the mobility of the spin label in the EPR spectra; τ_r rotation correlation time of the spin label

αS spin label positions	**components contributing in simulations**	**S87A (non-phosphorylated)**		**S87D (phosphorylated)**	
		τ_r (ns)	**contribution (%)**	**τ_r (ns)**	**contribution (%)**
SL 27	fast	0.4	5	0.4	5
	slow	2.5	90	2.8	93
	immobile	>50	5	>50	2
SL 56	fast	0.48	2	0.44	1
	slow	3.2	91	2.9	90
	immobile	>50	6	>50	8
SL 69	fast	0.3	2	0.3	14
	slow	2.2	98	2.5	86
	immobile	na	na	na	na

for error see table 2

Figure A1a shows the spectra of αS in the non-phosphorylated and Figure A1b in the phosphorylated form. In contrast to what we observe with LUVs, the spectra of αS27 and αS56 in the non-phosphorylated case (Figure A1a) are similar to those of the phosphorylated case (Figure A1b). The spectrum of αS69 in the phosphorylated case shows that the lines are narrower compared to its

non-phosphorylated counterpart. This is also evident from the simulation parameters shown in Table A1. Overall, αS shows stronger binding to SUVs than to LUVs (chapter 3) for the non-phosphorylated and phosphorylated variants, which is masking the effect of phosphorylation seen on LUVs.